



## Detection of early apple bruises using pulsed-phase thermography

Piotr Baranowski\*, Wojciech Mazurek, Barbara Witkowska-Walczak, Cezary Sławiński

*Institute of Agrophysics, Polish Academy of Sciences, ul. Doswiadczalna 4, 20-290 Lublin, Poland*

### ARTICLE INFO

#### Article history:

Received 1 December 2008

Accepted 18 April 2009

#### Keywords:

Apple bruise detection

Pulsed-phase thermography

Heat conduction in fruit

### ABSTRACT

The study is based on a hypothesis that internal defects and physiological disorders of fruit lead to changes in tissue thermal properties. During thermal stimulation, heterogeneities of thermal properties lead to the occurrence of thermal contrasts on the surface of fruit material, which can be successfully registered with the use of a thermographic device. A method was developed to detect apple bruising early using pulsed-phase thermography (PPT). In PPT the studied object is heated with an individual thermal pulse (most frequently a rectangular pulse) and the temperature decay on the surface is analysed on a pixel-by-pixel basis as a mixture of harmonic waves, thus enabling the computation of phase and amplitude images. The fast Fourier transform was used to obtain amplitudes and phasegrams of fruit heat response to defects occurring at different depths. The automatic segmentation procedure made it possible to select areas of bruised tissue in thermograms. A comparison of PPT results and visual inspection of bruising was performed, indicating high possibilities of the active thermography method for detecting defects up to several millimetres.

© 2009 Elsevier B.V. All rights reserved.

### 1. Introduction

In the process of apple sorting, an important problem is how to effectively detect early bruises. In spite of the fact that bruising is the reason for rejecting the highest number of fruit in sorting lines, manual sorting is still commonly used for detecting this defect (Leemans et al., 2002; Xing and Baerdemaeker, 2007). Bruising is defined as damage of fruit tissue as a result of external forces which cause physical changes of texture and/or chemical changes of colour, smell and taste (Mohsenin, 1986). Two basic effects of apple bruising can be distinguished, i.e. browning and softening of fruit tissue. The susceptibility of apples to mechanical damage depends on many factors, including soil cultivation, nutrition and weather conditions in the field during fruit growth (Woolf and Ferguson, 2000).

Existing sorting systems are not capable of effectively distinguishing fruit with bruising which occurs a short time before inspection. This is because the majority of these systems analyse reflected visible light and scattered near infrared radiation (up to 3  $\mu\text{m}$ ), thus they concentrate on detecting fruit browning, which in the case of fruit with early bruising may not occur or occur indistinctly (Samim and Banks, 1993; Ferguson et al., 1999; Xing et al., 2006). Even highly complicated visual sorting systems which perform a multispectral analysis of colour and use advanced procedures of image processing and analysis, including neural networks,

are not able to overcome this problem (Lu et al., 1999; Peng and Lu, 2005, 2006). The majority of current apple bruise detection methods show deficiencies in the case of dark skin colour or small surfaces of the bruise. Although it has been confirmed that X-ray imaging and magnetic resonance offer great potential possibilities for apple bruise detection (Chen et al., 1989; Zion et al., 1993; Thomas et al., 1995; Schatzki et al., 1997), these methods have not been implemented in existing sorting systems in spite of some ready-made prototype solutions, due to cost and methodological problems. The application of the near infrared spectroscopy method (NIR 700–2200 nm) has shown low effectiveness for bruise detection in the case of multicolour apples, e.g. 'Jonagold' or 'Braeburn', and for early bruising (Upchurch et al., 1994; Wen and Tao, 2000; Kleynen et al., 2003; Xing et al., 2005; Xing and Baerdemaeker, 2007).

Because of some shortage of existing methods for early apple bruise detection, there is growing interest in alternative non-destructive sorting methods. Preliminary investigations with the use of thermography for apple bruise detection indicate that this method has quite new possibilities, provided that the process of heat conduction in the fruit can be precisely identified and the mechanism of heat contrast development between the bruised part and sound areas on the fruit surface are understood (Lurie, 1998; Hellebrand et al., 2000; Roos, 2003; Walczak et al., 2003; Veraverbeke et al., 2006; Baranowski, 2008).

According to Varith et al. (2003), the temperature of the bruised apple surface is different to that in sound tissue areas of thermograms. This can be explained by differences in thermal properties (thermal diffusivity), caused by the loss of water in bruised areas

\* Corresponding author. Tel.: +48 81 7445061; fax: +48 81 7445061.  
E-mail address: [pbaranow@demeter.ipan.lublin.pl](mailto:pbaranow@demeter.ipan.lublin.pl) (P. Baranowski).

## Nomenclature

$A_n$	amplitude
$F_n$	discrete Fourier transform
$F(\nu)$	continuous Fourier transform
$f(t)$	continuous function of time
$j = \sqrt{-1}$	imaginary unit
$n$	frequency increment ( $n = 0, 1, 2, \dots, N$ )
$N$	number of discrete samples of $f(t)$
$t$	time (s)
$T$	temperature (K)
$\Delta t$	time resolution of images in a sequence (sampling interval) (s)
$w(t)$	truncation window (s)
Re	real part of Fourier transform
Im	imaginary part of Fourier transform
NETD	noise equivalent temperature difference
NIR	near infrared
PPT	pulsed-phase thermography
RH	relative humidity (%)
SSC	soluble solid content (%)
$\phi_n$	phase delay
$\nu$	frequency (Hz)
$\nu_c$	critical (Nyquist) frequency (Hz)
$\nu_s$	sampling rate (Hz)
$\Delta \nu$	frequency resolution of images in a sequence (Hz)

which have lower density than sound tissue. These authors made observations of apple temperature after apples sustained severe bruises (dropped from a height of 0.46 m) and were stored at a temperature of 25 °C and air humidity of 50%.

Two approaches exist in thermographic studies for non-destructive defect detection: passive and active. Passive thermography consists of measurement of radiation temperature under conditions of natural differentiation between studied objects and surrounding air, while active thermography requires an external source of heating of the studied object (Więcek and Zwolenik, 1998; Maldague, 2001; Ibarra-Castanedo and Maldague, 2004; Meola and Carlomagno, 2004). The main advantage of active thermography is the possibility to detect defects occurring beneath the surface and to evaluate the defect depth on the basis of heat pulse characteristics and changes in time of temperature distribution on the studied object. Passive thermography was used by Baranowski et al. (2005) for bruise detection in three apple varieties, ‘Jonagold’, ‘Ligol’ and ‘Gloster’. The patterns of temperature changes on the surface of the bruised fruit showed that, with respect to the investigated varieties, the temperature differences between bruised and sound tissue changed from 0.5 °C to 1.5 °C. The experiment was performed at an ambient temperature of 25 °C. It was also found that effective bruise detection by using passive thermography could be done about 48 h after defect occurrence. The highest temperature differences were noted for ‘Jonagold’ fruit and the lowest for ‘Gloster’, which was a result of differences in apple firmness between these varieties.

In the present paper, a hypothesis is put forward that the application of active thermography will enable identification of thermal contrast between bruised and sound tissue in apples in early stages (up to several hours) after the occurrence of bruising. Because this approach is quite new in studies on fruit, methodological aspects had to be considered, including the choice of optimal heat pulse parameters (power and heating time) and sequence registration parameters (frequency of images in the sequence and total number of images in a sequence).

The aim of the study was to examine applicability of active thermography (PPT) for detecting early apple bruising, in particular: distinguishing bruised and sound areas on the apple surface on the basis of heating curves and elaborating an effective segmentation procedure; comparing visible light imaging with thermographic methods for detecting early bruises; checking whether amplitude and phase analyses of fruit response to the stimulating heating pulse performed by PPT are capable of providing information about the bruise depth.

## 2. Materials and methods

‘Jonagold’, ‘Champion’ and ‘Gloster’ apples (*Malus domestica* Borkh) were collected from the same orchard directly after hand harvest in 2007 and then, before thermographic measurements, they were stored for 15 h at 21 °C and 85% RH. A total of 150 apples (50 for each variety) of uniform size (equator diameter between 77 mm and 82 mm) were used in the experiment.

In order to check whether active thermography enables distinguishing of bruises down to various depths, a specific bruising procedure was applied. Two positions on the surface of each apple were chosen for bruising, both lying in the longitudinal line: the first one was half way between the calyx and the pedicle, and the second half way between the equator and the pedicle end. A plastic roller with a diameter of 10 mm and a thickness of 1 mm was put successively in these two positions and a cylindrical weight of 0.2 kg was dropped (the contact surface was the base of the cylinder) from a height of 400 mm on the central position (a deeper bruise) and from a height of 200 mm on the pedicle end position (a shallower bruise). The fruit were then stored at room temperature for 1 h before thermographic bruise assessment.

To calculate fruit bulk density, before each thermographic acquisition, each apple was weighed with an electronic digital Mettler XS1003S balance (Mettler Inc., Switzerland), operating at a capacity of up to 1000 g with readability of 0.001 g and the fruit volume was obtained through the measurement of water volume which was displaced by the fruit. Additionally, after the thermographic inspection, fruit firmness was determined using a penetrometer, model FT 327 (Facchini srl, Alfonsine, Italy), equipped with a tip 11.3 mm in diameter. Three measurements of firmness were made on each fruit, in the pedicle area, the middle part of the apple and in the calyx area. The means of these three firmness readings were expressed in *N*.

Soluble solids concentrations (SSCs) were determined using an Abbe refractometer (Zeiss Jena, Germany), at an ambient temperature of 20 °C. For each apple, two measurements of SSC were made at opposite sides of the fruit and were expressed as %.

The fruit maturity stage was assessed by the standard starch–iodine test to document starch disappearance. A rating scale of 1–6 was used according to the procedure described in Pennsylvania Tree Fruit Production Guide (2005) where 1 is full starch and 6 free of starch.

A special measuring system for active thermography was designed, consisting of a thermographic camera, two halogen lamps (500 W each) fixed on a tripod, a system for controlling the heat pulse time as well as registration parameters and external conditions in the thermostated laboratory.

In the study, a thermographic camera VIGOCam v50 (Vigo Systems, Warsaw, Poland) was used. It is sensitive in the spectral range of 8–14 μm. The camera is constructed with the use of a 384 × 288 microbolometric detector array. The system’s thermal sensitivity NETD is 0.08 °C at 30 °C of the object temperature. The spatial resolution of the camera is 1 mrad. It works with a frame rate of 60 Hz. The connection with a PC computer is possible via USB or Ethernet ports. A lens with an angular field of view of 22° was used. The thermographic camera is additionally equipped

with a visible light photo camera which takes photos of the examined surface at selected moments of thermographic registration. In this way, thermographic and visible light images can be compared.

The measurement of radiation temperature of the apples was done under controlled external conditions. All the measurement series were performed at an air temperature of 21 °C and relative humidity of 60% in daylight. The distance between the camera lens and the apple surface was 0.5 m. The halogen lamps were situated at a distance of 0.3 m from the apple surface and the distance between the centres of both lamps was 0.38 m.

To compare the visibility of bruises in thermal images with their visibility and real sizes in visible light, the photos of the investigated surfaces were examined, obtained directly after switching on the halogen lamps during thermographic registration and after skin removal. Bruise visibility was evaluated using a rating scale of 0–5 proposed by Studman et al. (1997). In this scale, 0 refers to “no bruising visible” and 5 to “bruising very visible”. Then, each apple was cut through the centre of both bruises along the calyx–stem axis to measure the bruise depth. For bruise volume calculations, the method described by Holt and Schoorl (1977) was used, which requires the measurement of the curvature of the fruit in both equatorial and polar directions.

On the basis of the knowledge of thermal properties of fruit tissue (Mohsenin, 1980) and the depth of the bruise (ranging in this case between 1 mm and 4 mm), a frame rate of 15 images/s and a number of frames in each sequence equal to 500, which corresponded to an acquisition time of about 33 s, was chosen. Another problem important for proper design of the experiment with active thermography was to select appropriate pulse power. This parameter mainly depends on thermophysical and structural properties of the studied object. The power of the stimulating signal should be

sufficient to ensure heat transfer into a specific depth at a specific speed.

Thermal images were registered and processed on a preliminary basis using firmware software THERM v50 (Vigo Systems, Warsaw, Poland). This software, along with numerous functions for thermographic data processing, enables export of individual images and whole sequences in the text format to other programs. The procedure of image segmentation to select bruised areas was performed by creating a separate plugin in ImageJ software developed at the National Institutes of Health, Bethesda, MD, USA (Rasband, 1997–2007). Fast Fourier transform for PPT and analysis of ampligrams and phasegrams were carried out using a MATLAB script IR\_View v.1.7 developed at the Electrical and Computing Engineering Department, Laval University, Quebec City, Canada.

To analyse the response of the object to the heat pulse, images obtained during the heating process (during the heat pulse duration) and images of cooling (after the heat pulse) were studied separately.

Particular thermal images of the apple surface were subjected to computer analysis to automatically select the areas in each image representing the surfaces of particular bruises. To do this, raw images obtained from the thermographic camera with specific registration parameters (ambient temperature, air temperature, fruit surface emissivity, distance between the camera and the fruit surface) were exported as text files to the ImageJ programme.

The first stage of image processing was scaling which consisted of determination of the spatial scale of the image in calibrated units (cm). A segment was created coming between two opposite edges of the basement of known size on which the investigated fruit was placed. On the basis of the pixel number along this segment and the known length of the basement, the programme automatically calculated all distances in the chosen unit (cm).

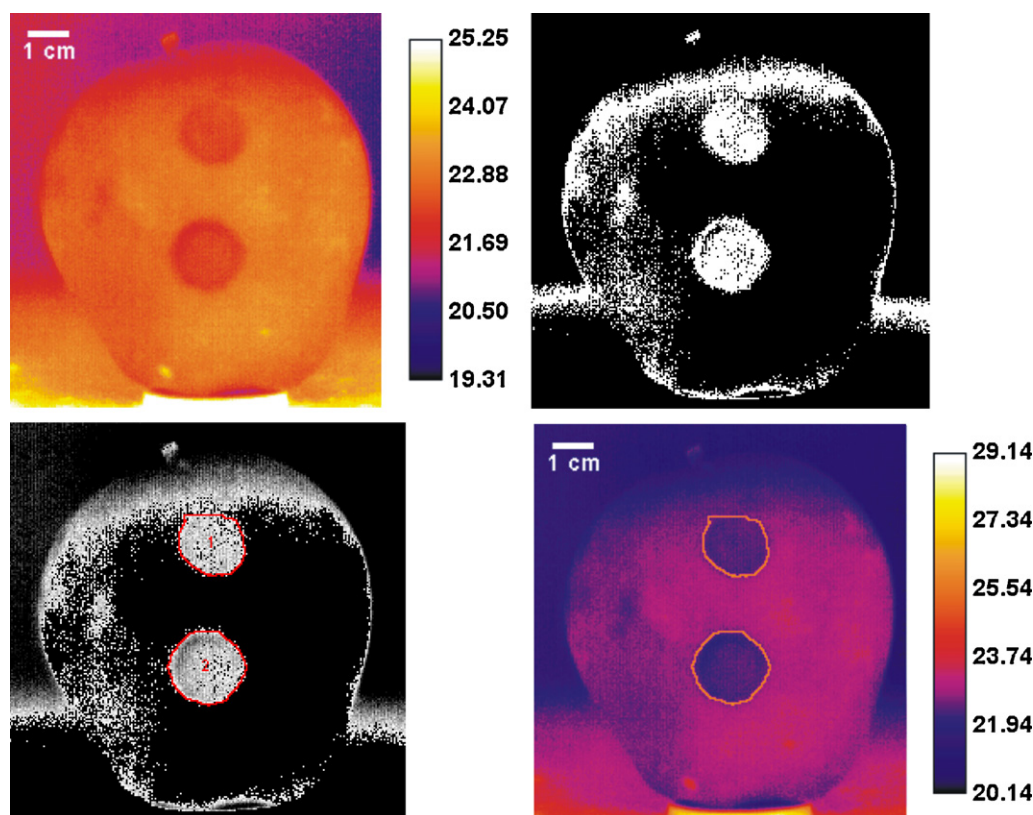


**Fig. 1.** Presentation of subsequent stages of the segmentation procedure for a thermal image with bruise areas: the scaled original thermal image after applying correction of contrast and brightness (upper left), the effect of thresholding of the image (upper right), the thresholded image with selected edges of bruised areas after the creation of masks and automatic numeration (lower left), the original thermal image with masks (lower right).



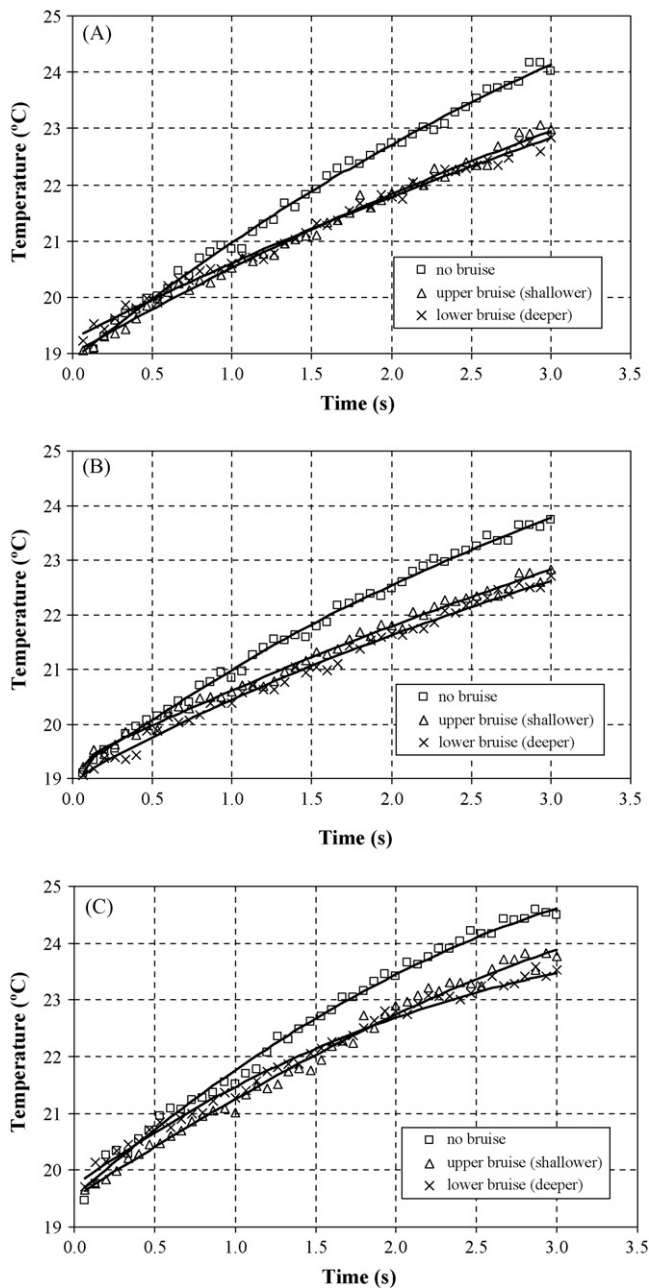


**Fig. 2.** Increase of average temperature for two bruised areas and sound tissue area for: 'Jonagold' (A), 'Champion' (B) and 'Gloster' (C) fruit.

The next step of the segmentation procedure was the preparation of the image for automatic thresholding (Ridler and Calvard, 1978). The brightness and contrast of the image were fixed on the basis of the histogram analysis of a selected part of the image covering the apple. The optimization of image brightness and contrast consisted of setting the range of temperatures for pixels of the investigated area, to eliminate sub-ranges which do not refer to temperature values in the investigated area. Noise reduction in the

image was obtained by using a median filter which changed the temperature value in each pixel of the image into the median value of neighbouring pixels.

To sharpen the edges of the bruised areas, an additional procedure of histogram equalization was applied. Due to the complicated scene of the studied images, it was decided to use the recursive segmentation method which is based on image thresholding. In this method, histograms are calculated, associated with image attributes such as shade, saturation, brightness and others. Then a histogram is selected with the most distinctive pick. It enables determination of the attribute according to which the segmentation is performed. This procedure was repeated many times for previously selected areas and other parts of the image until the last area of the specified properties was selected. The segmentation obtained as a result of this procedure is characterised by high detail and precision.

To analyse the sequences of thermograms obtained after the heat pulse occurrence, an active thermography method was used. Firstly, the behaviour of temperature distribution on the fruit surface was studied during the heat pulse occurrence, which lasted 3 s. Secondly, the pulsed-phase thermography (PPT) method was used to study the thermal contrasts on the apple surface between bruised and sound tissue after the heat pulse occurrence.

In the PPT method, an individual rectangular heat pulse is used and the characteristic thermal response of the object to this pulse is analysed. The heat response signal can be presented as a superposition of the number of waves, each having different frequency, amplitude and phase delay. It is done by the use of the Fourier transform algorithm. The continuous Fourier transform is expressed by the infinite integral of exponential functions:

$$F(\nu) = \int_{-\infty}^{\infty} f(t)e^{-j2\pi\nu t} dt \quad (1)$$

where  $j^2 = -1$ . In the case of sampled (discrete) signals, a faster and more effective discrete Fourier transform is used. When a finite series of signal samples ( $T_0, T_1, T_2, \dots, T_{N-1}$ ) is analysed, it can be transformed into a harmonic series ( $F_0, F_1, F_2, \dots, F_{N-1}$ ) by using the following formula:

$$F_n = \sum_{k=0}^{N-1} T_k e^{-j2\pi nk/N} = \text{Re}_n + j\text{Im}_n \quad (2)$$

where  $\text{Re}$ ,  $\text{Im}$  are the real and imaginary parts of the transform, respectively,  $j$  is an imaginary unit,  $n$  is the number of harmonic components ( $n=0, 1, \dots, N$ ),  $k$  is the value of the signal sample. In PPT, the so-called algorithms of fast Fourier transform can be used, e.g. the Cooley–Tukey algorithm.

The real and imaginary parts of Fourier transform are used to calculate the amplitude and the phase:

$$A_n = \sqrt{\text{Re}_n^2 + \text{Im}_n^2} \quad (3)$$

$$\phi_n = \tan^{-1} \left( \frac{\text{Im}_n}{\text{Re}_n} \right) \quad (4)$$

In the sequence of  $N$  thermograms of the studied surface, there are  $N/2$  useful frequency components. The other half contains interference information which can be safely rejected. In this study the number of images in each sequence was chosen in such a way that

**Table 1**

Quality characteristics of the studied apples. The standard deviation is given in parentheses under the respective quantity value.

Apple variety, $N$ —number of bruised fruit	Mean bulk density ( $\text{kg m}^{-3}$ )	Soluble solid content (%)	Firmness ( $N$ )	Generic starch–iodine index
'Jonagold', $N=50$	859.3 (4.4)	13.2 (0.5)	62.2 (2.2)	4.6
'Champion', $N=50$	863.6 (3.8)	13.8 (0.8)	59.1 (1.6)	4.1
'Gloster', $N=50$	852.4 (4.2)	14.1 (0.6)	57.4 (1.5)	5.2

**Table 2**  
Bruise area, depth and volume obtained from visual inspection and bruise area evaluated by thermographic examination of the investigated varieties. The standard deviation is given in parentheses under the respective quantity value.

Apple variety, <i>N</i> —number of bruised fruit	Mean drop height (mm)	Visible light inspection		Mean bruise area (skin off) (2 h after bruising) (mm <sup>2</sup> )	Mean bruise area (skin off) (14 h after bruising) (mm <sup>2</sup> )	Mean bruise depth (mm)	Mean Bruise Volume (mL)	Thermographic inspection Mean bruise area (first hot thermal image) (mm <sup>2</sup> )
		Mean bruise area (skin on) (mm <sup>2</sup> )	Mean bruise area after bruising) (mm <sup>2</sup> )					
'Jonagold', <i>N</i> = 50	200	60.4 (1.1)	41.6 (1.7)	61.9 (1.6)	61.9 (1.6)	1.2	50.5 (2.7)	64.5 (2.0)
	400	70.5 (1.9)	62.3 (2.2)	74.1 (2.1)	74.1 (2.1)	3.6	102.2 (4.0)	76.3 (1.9)
'Champion', <i>N</i> = 50	200	49.6 (1.3)	40.5 (1.8)	60.5 (1.5)	60.5 (1.5)	1.1	49.7 (2.8)	62.1 (1.7)
	400	70.8 (2.0)	61.7 (2.6)	72.7 (2.4)	72.7 (2.4)	3.5	101.1 (3.6)	74.5 (2.3)
'Gloster', <i>N</i> = 50	200	56.8 (1.9)	48.3 (1.6)	63.9 (2.0)	63.9 (2.0)	1.5	56.8 (3.8)	64.5 (1.5)
	400	75.2 (2.8)	68.5 (2.3)	78.5 (2.7)	78.5 (2.7)	3.9	105.2 (5.3)	78.3 (2.1)

the value of fruit temperature at the end of each sequence was close to the ambient temperature. Each registered sequence contained about 500 images collected with the time step of 0.07 s. The amplitude and phase analysis of thermograms enable important information to be obtained about the process of heat penetration within the studied objects, the depth and size of subsurface defects and the thermal properties of the object. However, to perform this analysis in a proper way, certain conditions should be fulfilled. Special attention must be paid to establish how fast and how long the continuous temporal signal of the surface response to the heating pulse needs to be sampled. The frame rate and the acquisition time are limited by the maximum storage capacity of the infrared system. Furthermore, the choice of the frame rate strongly depends on the thermal properties of the specimen (high conductivity materials require a faster frame rate). The choice of registration time significantly influences the phase characteristics of thermograms. The best way not to lose important phase information from thermograms is to use long times of registration of thermal response of the object to the pulse in order to let the surface temperature return to its initial value, corresponding to the moment before the pulse application.

### 3. Results and discussion

All the thermal images of the apples with bruises were processed to select areas of defects automatically. An example of successive stages of automatic segmentation of an image is shown in Fig. 1. The thermal image obtained after correction of brightness and contrast of the original thermogram from the camera with scale and isotherm bars is presented in the upper left corner of Fig. 1. The automatic correction of the contrast and brightness was a preliminary stage of preparation of the thermal images for the automatic segmentation procedure. The procedure of selecting edges of the bruised regions was performed using the Particle Analysis procedure included in ImageJ software. It works by scanning the image or selection until it finds the edge of an object, following the assumed criteria of size and circularity of the bruised regions. Areas outside the range specified in the size and circularity fields are ignored. The formula for circularity is  $4\pi$  (area/perimeter<sup>2</sup>). The effect of the thresholding procedure and of the creation of masks surrounding the bruised areas is shown in the upper left and lower right corners of Fig. 1. The thermal image with masks of the bruised areas (the lower right corner of Fig. 1) formed the basis for the analysis of radiation temperature of damaged and sound tissue.

For all pixels in two selected areas (bruised tissue) and additionally for pixels within the area covering the rest of the fruit surface (sound tissue), basic statistical values were derived. It enabled evaluation of temperature differentiation between the bruised and sound areas for fruit of the three apple varieties.

In the first stage of the study, the sequences of fruit surface thermograms were analysed during the heating process (the halogen lamps switched on for 3 s) to find whether any thermal contrasts were visible between the bruised and sound areas. The results of this analysis are presented in Fig. 2. The temperature rise patterns show that at the beginning of fruit surface heating the temperature differences between the sound and bruised areas as well as between the shallower and deeper bruises are close to 0 °C. It indicates that passive thermography (no heat stimulation) cannot be used for early bruise detection. Considerable differentiation of radiation temperature between the bruised and non-bruised areas occurred after the first second of heating the apple. The highest temperature differences between the bruised and sound areas were noticed directly before breaking off the heat pulse. For all the 50 fruit of each variety, they ranged between 0.9 °C and 1.5 °C for 'Jonagold', 0.9 °C and 1.8 °C for 'Champion', and between 1.0 °C and 2.1 °C for 'Gloster' fruit. The differences in radiation temperature during the heating

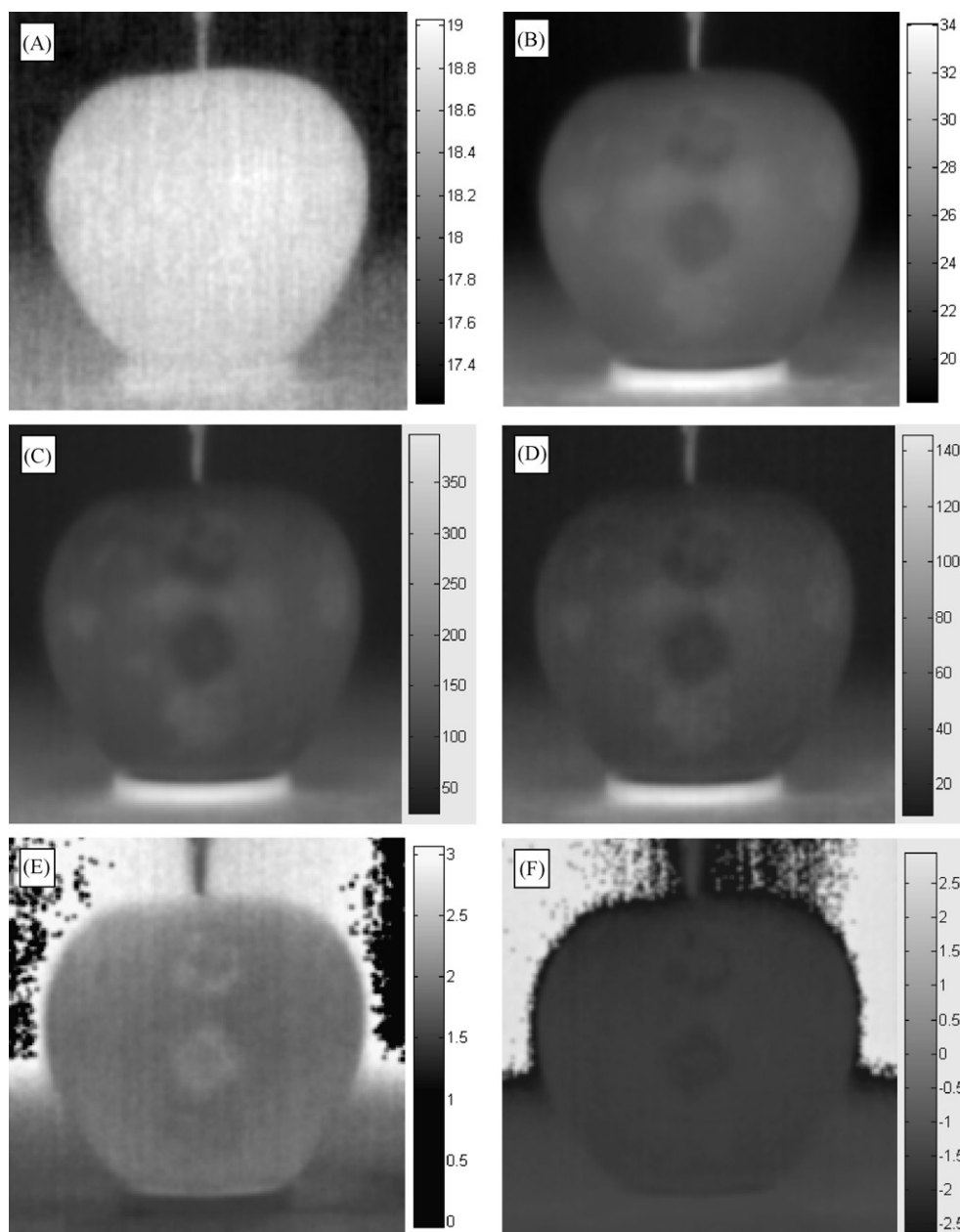


**Fig. 3.** Thermograms of a 'Champion' apple with two bruised areas obtained by the PPT method with the indication of shallower (2 m) and deeper (up to 4 mm) bruises. Subsequent images represent: (A) cold image, (B) the first thermogram after the heat pulse, (C and D) ampligrams, and (E and F) phasegrams. Time of pulse 3 s.

process between the deeper and shallower bruises were very small and did not exceed  $0.4^{\circ}\text{C}$ . These results indicate that the analysis of radiation temperature for the duration of the heating pulse allows bruised areas to be distinguished, however it is impossible to distinguish deeper and shallower bruises.

The study did not reveal statistically significant correlations between rate of fruit surface temperature increase during the heating pulse occurrence and bulk density. It probably resulted from the fact that the density values for all 150 apples were within a relatively narrow range. The highest differences in bulk density mean values were noticed between 'Gloster' and 'Champion' apples and they reached  $11.2\text{ kg m}^{-3}$ , and the lowest,  $4.3\text{ kg m}^{-3}$ , between 'Champion' and 'Jonagold'. The highest mean value of apple flesh firmness was noted for the 'Jonagold' variety,  $62.2\text{ N}$ , whereas for the other two varieties it was equal to  $57.4\text{ N}$  ('Gloster') and  $59.1\text{ N}$  ('Champion'). Additionally, the SSC did not vary significantly between the varieties and its mean values for the respective varieties were

equal to  $13.2\%$  ('Jonagold'),  $14.1\%$  ('Gloster') and  $13.8\%$  ('Champion'). 'Gloster' apples had the highest maturity index (ready for fresh market), whereas 'Jonagold' and 'Champion' apples possessed a slightly lower level of maturity (ready for long term storage) (Table 1).

On the basis of visible light and thermal images of the fruit surface, a comparison was made between mean bruise areas for all the apples (Table 2). The mean areas of early bruise measured by the visible light method 2 h after bruising were significantly smaller than those measured after 14 h, both for deeper and shallower defects. For the studied varieties, the shallower defects were projected on the fruit surface with smaller mean areas than the deeper defects. It was observed that the bruised surfaces with skin on, for the particular varieties and bruise depths, had higher mean surface areas than the respective surfaces without skin. The mean bruise areas obtained from thermographic images were close to those measured from visible light images obtained 14 h after bruising. In this case,

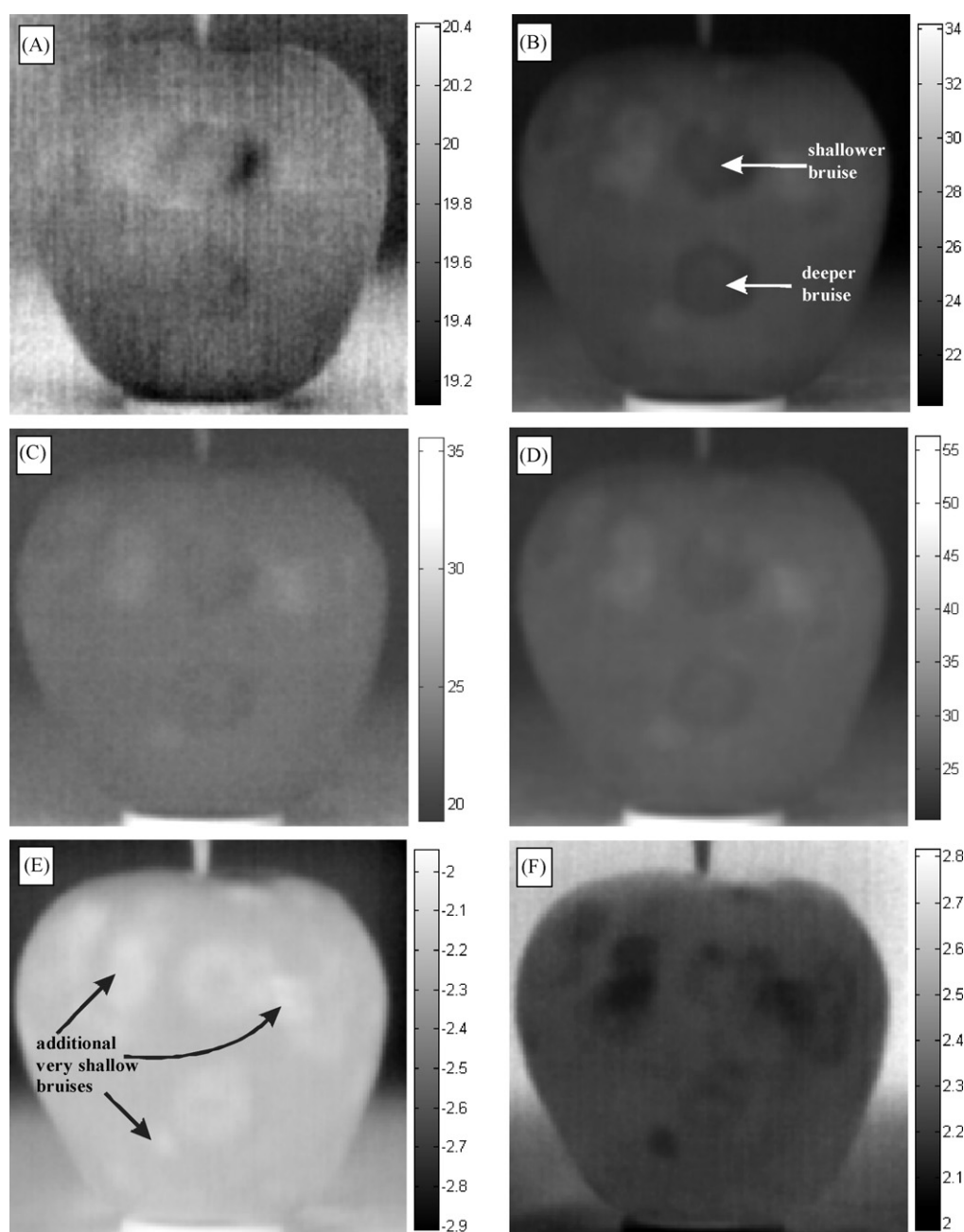


**Fig. 4.** Thermograms of a 'Gloster' apple with two bruised areas obtained by the PPT method. Subsequent images represent: (A) cold image, (B) the first thermogram after the heat pulse, (C and D) amplitograms, and (E and F) phasegrams. Time of pulse 3 s.

the differences between the mean areas of the deeper and shallower bruises were much smaller than those observed by visible light inspection 2 h after bruising. On the basis of Table 2, visible light inspection of early bruise (2 h after bruising) does not enable detection of damaged areas of fruit tissue and thermographic inspection in this early stage after bruising gives a chance to detect bruised areas which can be seen in visible light images many hours later. The results in Table 2 also show that the mean bruise depth and the mean bruise volume values for the respective drop heights were the highest for 'Gloster', this being probably connected with the lowest mean bulk density and firmness of this variety.

Because the heating curves did not allow us to distinguish between deeper and shallower bruises, it was decided to analyse radiation temperature patterns after the end of the heat pulse. By using IR.View, the registered sequences were analysed, and

amplitograms and phasegrams for various frequencies were created. The results of this analysis are presented in Figs. 3 and 4, where thermograms marked with A are the images of the apples before heat pulse extinction (cold image). Fruit bruises are not visible on these thermograms, which indicates that passive thermography cannot be used for detection of early bruises. Thermograms B in these figures are the first images obtained after stopping the heat pulse. In these thermograms, bruised areas are easily distinguishable as colder regions on the apple surface. By comparing thermograms A and B, it is possible to evaluate how large an increase of temperature in particular parts of the fruit occurred as a result of the heat pulse. To eliminate signal distortion associated with the noise from the camera, differential images between the first one in the sequence after stopping the heat pulse and cold images were created and they were the basis for amplitude and phase analysis.



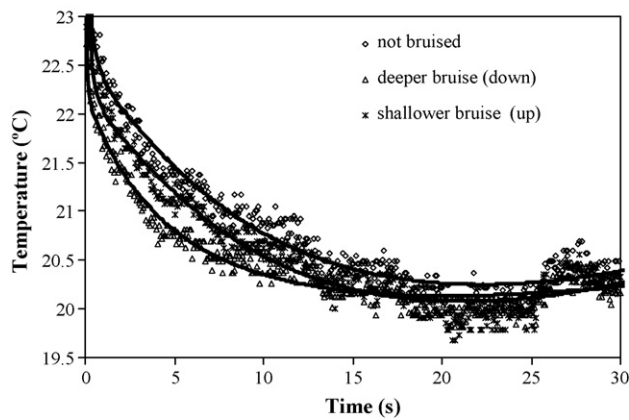


**Fig. 5.** Patterns of radiation temperature changes on the surface of sound and two bruised parts of a 'Champion' apple (the upper bruise reaches 2 mm and the lower bruise up to 4 mm under the skin).

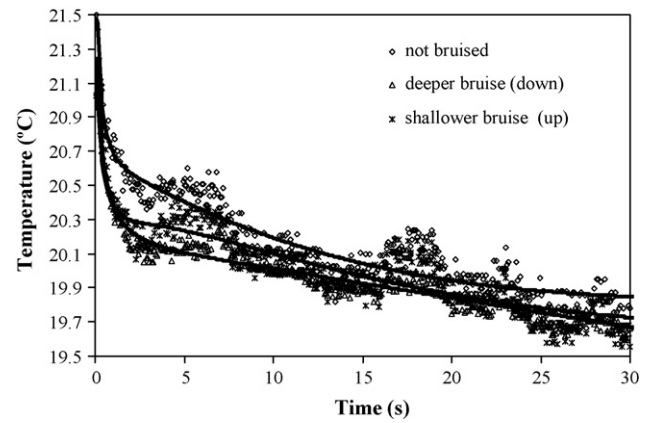


**Fig. 6.** Patterns of radiation temperature changes on the surface of sound and two bruised parts of a 'Gloster' apple (the upper bruise reaches 2 mm under the skin and the lower bruise up to 4 mm).

Figs. 3 and 4 show thermograms of 'Champion' and 'Gloster' fruit. In these thermograms, the lower bruise was deeper, 4 mm, and the upper bruise shallower, 2 mm. The duration of the heating pulse was 3 s and the pulse power was 1000 W. The bruises in these thermograms were recorded 2 h after their creation. The highest thermal contrasts between the bruised and sound tissue areas were observed for 'Gloster' apples (Fig. 4).

Thermograms C and D in Figs. 3 and 4 are amplitograms, whereas thermograms E and F are phasegrams for two different frequencies. These images were obtained with the use of discrete Fourier transform according to Eq. (3). These phasegrams and amplitograms relate to two chosen frequencies at which the most significant contrasts were observed. As can be seen from these images, the amplitude and phase analyses help to derive additional information from the thermograms about the defect distribution. The amplitude analysis enables, in some cases, better contrast between bruised and sound tissue to be obtained than from individual thermal images. The phase analysis of thermogram sequences is especially useful for the detection of defects at various depths beneath the fruit skin. It not only allows elimination of distortion of radiation temperature distribution resulting from unhomogenous heating by halogen lamps, but also identification of defects at various depths for component frequencies of the heat response. Shallower defects on phasegrams were obtained for higher frequencies, whereas deeper defects on phasegrams were for lower frequencies (Fig. 4E and F). The first one was obtained for the frequency of 0.1 Hz, while the second for 0.3 Hz. In phasegram 4E, deeper defects are mainly distinguished and in phasegram 4F the contrast comes from shallower defects of browning tissue beneath the apple surface, confirmed by cutting the apple after the measurement.

In Figs. 5 and 6 the courses of temperature measured with the thermographic device for the pixels of the image with a bruise

defect and without bruising as well as the corresponding polynomial curves of the 4th degree fitted into the measuring data, are presented. The curves for the pixels of bruised tissue are characterised by a higher decrease in temperature in the first phase of cooling. It was also noticed that the considerable differences in the temperature courses exist between the pixels over the areas of defects occurring at various depths. This result indicates that the analysis of the cooling curve for the pixels of the thermal image of apple surface is useful for distinguishing pixels of the defects of various depths. The oscillations in the temperature versus time were observed in Figs. 5 and 6 which were probably the result of a non-uniform heat transfer within the fruit flesh as a result of the complicated three-phase structure of fruit tissue. It is an interesting problem for future studies.

The temperature profiles presented in Figs. 5 and 6 can be used for distinguishing between shallower and deeper bruises, however, in general, non-uniform heating, reflections from the environment, surface emissivity variations and surface geometry all have an impact on temperature profiles. Quantification of defect depths using thermal data would be difficult to accomplish in these conditions. Phase, on the other hand, is practically unaffected by above-mentioned factors. Therefore, further study in this paper is mainly focussed on phase analysis.

The main sampling and truncation parameters in time and frequency domains, which were selected for this study on the base of methodology elaborated by Ibarra-Castaneda and Maldague (2004), are presented in Table 3. For the selected sampling and truncation parameters the analysis of the relation between the phase of the thermal response on the surface of fruit and the frequencies of particular components of the response signal (phase profiles) was performed. The results for exemplary shallower bruises (A) and deeper bruises (B) for the apples are presented in Fig. 7. For each

**Table 3**

Sampling and truncation parameters used in the study in time and frequency domains.

Parameter	Time	Frequency
Image frame rate		$\nu_s = 15$ images/s
Resolution	$\Delta t = \frac{1}{\nu_s} = \frac{1}{15} \text{ s} \approx 0.067 \text{ s}$	$\Delta \nu = \frac{1}{w(t)} = 0.03 \text{ Hz}$
[5pt] Truncation window	$w(t) = N \Delta t = 500 \cdot \frac{1}{15} \approx 33, 3 \text{ s}$	$\nu_{\max} = \frac{1}{2 \Delta t} \approx 7.5 \text{ Hz}$
Sampling points	$N = 500$	$\frac{N}{2} = 250$
[5pt] Single $n$ th element value	$t_n = n \Delta t$	$\nu_n = \frac{n}{N \Delta t} = \frac{n}{500(1/15)} = \frac{n}{33.3 \text{ s}}$
Minimum value	$t_1 = \Delta t$	$\nu_1 = \frac{1}{N \Delta t} = \Delta \nu$
Maximum value	$t_N = t_0 w(t), t_0 = \text{initial time}$	$\nu_N = \frac{1}{2 \Delta t} = \frac{\nu_s}{2} = \nu_c$



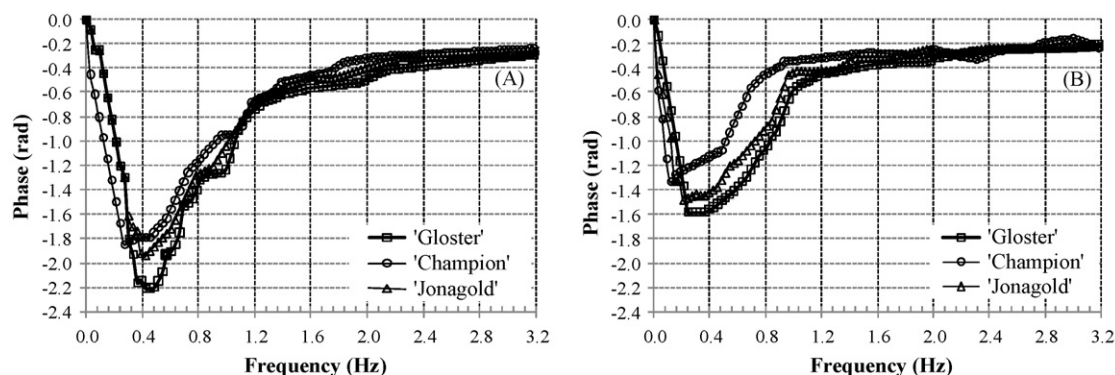


Fig. 7. Change of phase for various frequencies of thermal response in shallower (A) and deeper (B) bruised areas in apples of the three varieties.

variety there exists the most suitable frequency for which discrimination between shallower and deeper bruises is the most effective. This frequency corresponds to a characteristic decrease of phase (a minimum phase peak). The deeper the bruise the smaller the frequency value of the minimum phase peak. To improve visibility of the region in Fig. 7 in which the inflection points occur, a limited range of frequencies (0–3.2 Hz) is presented. In the range of the other frequencies the phase profiles tend asymptotically to a zero-phase value and discrimination between deeper and shallower bruises is impossible. It is apparent from Fig. 7 that clear depth discrimination can be performed in the range from “0” to a limiting frequency, which in the case of the phase profiles presented in Fig. 7 is equal to about 2 Hz. From this limiting frequency to the maximum frequency  $\nu_{\max}$  (7.5 Hz) phase values of the points belonging to apples of various depths are all mixed together and not depth distinction can be made.

Some differences of phase values in minimum peak points occur between fruit varieties. Both for deeper and shallower bruises the lowest values of phase in minimum peak points were noticed for ‘Gloster’ fruit.

The linear correlation regression models were created for early bruise depths and the component frequencies at which the minimum peak points occurred in the phase profiles. The respective correlation equations are presented in Fig. 8. The coefficients of determination  $R^2$  for these models were: ‘Gloster’, 0.98, ‘Jonagold’, 0.96 and ‘Champion’, 0.96. The limited number of points (8) in Fig. 8 comes from the limited range of bruise depth values measured in the experiment. This range was slightly different for each variety.

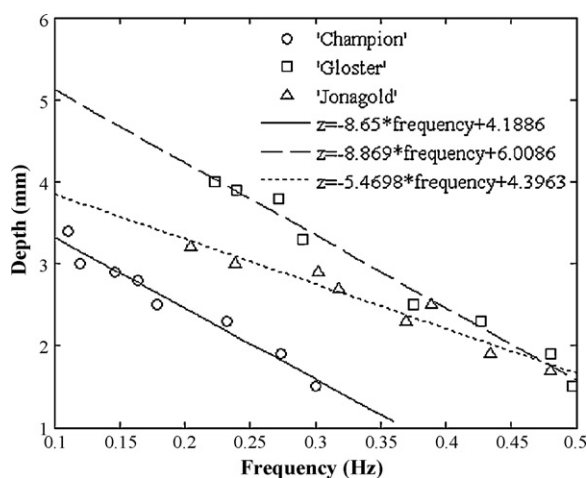


Fig. 8. Correlation between bruise depth and frequency of thermal response for which the highest contrast exists in phasegrams between bruised and sound areas: (A) ‘Jonagold’, (B) ‘Champion’, and (C) ‘Gloster’.

The frequencies at which the bruises of the depths from 1 mm to 4 mm can be detected are within the range from 0.1 Hz to 0.5 Hz. The regression lines obtained for ‘Champion’ and ‘Gloster’ are nearly parallel (slope 8.65 and 8.87, respectively) whereas the directional coefficient for ‘Jonagold’ is smaller (5.47).

The thermographic system and methodology developed for early bruise detection presented in this paper can support existing ‘computer vision’ systems of fruit quality evaluation. In order to implement this system in fruit sorting lines, it is necessary to solve some technical problems which have not been considered in this paper. They relate to the creation of stable thermal conditions during thermographic measurements in a sorting line, an effective analysis of thermograms of the whole surface of a quickly moving fruit, analysis of many fruits at the same time, etc.

#### 4. Conclusions

The investigations have shown the usefulness of active thermography for detection of early bruises in apples. The hypothesis has been confirmed that inner defects of fruit tissue, leading to local changes of thermal properties, are responsible for obtaining thermal contrasts between bruised and sound areas on the fruit surface, which can be successfully registered by using the PPT method.

An effective segmentation procedure has been elaborated to automatically distinguish bruised areas on thermograms. Thermographic inspection in the early stage after bruising enables detection of bruise areas which are seen in visible light images many hours later.

With the use of PPT method it is possible to distinguish in thermogram sequences bruises reaching various depths under the skin. Linear correlation exists between the depth of bruising and frequency of the thermal response.

#### Acknowledgements

The authors gratefully acknowledge the financial support of the Polish Ministry of Science and Higher Education under the Project No. N N310 3062 34 for the years 2008–2009. We also wish to thank Professor Hamlyn G. Jones of the Dundee University at SCRI for his encouragement, discussion and valuable comments.

#### References

- Baranowski, P., Lipecki, J., Mazurek, W., Walczak, R.T., 2005. Detection of mechanical defects in apples with the use of thermography (in Polish). *Acta Agrophys.* 125, 19–30.
- Baranowski, P., 2008. Radiation temperature of chosen fruit and seed as a parameter of their quality evaluation (in Polish). *Acta Agrophys.*, 159.
- Chen, P., McCarthy, M.J., Kauten, R., 1989. NMR for internal quality evaluation of fruits and vegetables. *Trans. ASAE* 32, 1747–1753.

- Ferguson, I., Volz, R., Woolf, A., 1999. Preharvest factors affecting physiological disorders of fruit. *Postharvest Biol. Technol.* 15, 255–262.
- Hellebrand, H.J., Linke, M., Beuche, H., Herold, B., Geyer, M., 2000. Horticultural Products Evaluated by Thermography. *AgEng, Warwick*, pp. 26–126.
- Holt, J.E., Schoorl, D., 1977. Bruising and energy dissipation in apples. *J. Texture Stud.* 7, 421–432.
- Ibarra-Castaneda, C., Maldague, X.P., 2004. Pulsed phase thermography reviewed. *QIRT J.* 1, 47–70.
- Kleynen, O., Leemans, V., Destain, M.F., 2003. Selection of the most efficient wavelength bands for 'Jonagold' apple sorting. *Postharvest Biol. Technol.* 30, 221–232.
- Leemans, V., Magin, H., Destain, M.F., 2002. On-line fruit grading according to their external quality using machine vision. *Biosyst. Eng.* 83, 397–404.
- Lu, R., Chen, Y.R., Park, B., 1999. Hyperspectral imaging for detecting bruises in apples. In: *ASAE Annual International Meeting, Toronto, Canada, July 18–21, Paper No. 99-3120*.
- Lurie, S., 1998. Postharvest heat treatments. *Postharvest Biol. Technol.* 14, 257–269.
- Maldague, X.P., 2001. *Theory and Practice of Infrared Technology for Nondestructive Testing*. John Wiley & Sons, New York.
- Meola, C., Carlomagno, G.M., 2004. Recent advances in the use of infrared thermography. *Meas. Sci. Technol.* 15, 27–58.
- Mohsenin, N.N., 1980. *Thermal properties of foods and other agricultural materials*. Gordon Breach.
- Mohsenin, N.N., 1986. *Physical properties of plant and animal materials*. Gordon Breach.
- Peng, Y., Lu, R., 2005. Modelling multispectral scattering profiles for prediction of apple fruit firmness. *Trans. ASAE* 48, 235–242.
- Peng, Y., Lu, R., 2006. An LCTF-based multispectral imaging system for estimation of apple fruit firmness. Part II. Selection of optimal wavelengths and development of prediction models. *Trans. ASAE* 49, 269–275.
- Pennsylvania Tree Fruit Production Guide, 2005. <http://tfpg.cas.psu.edu>.
- Rasband, W.S., 1997–2007. *ImageJ*. US National Institutes of Health, Bethesda, MD, USA, <http://rsb.info.nih.gov/ij/>.
- Ridler, T.W., Calvard, S., 1978. Picture thresholding using an iterative selection method. *IEEE Trans. Syst. Man Cybern.* 8, 630–632.
- Roos, Y.H., 2003. Thermal analysis, state transitions and food quality. *J. Therm. Anal. Calorim.* 71, 197–203.
- Samim, M., Banks, N.H., 1993. Color changes in bruised apple fruit tissue. *N. Z. J. Crop Hort. Sci.* 21, 367–372.
- Schatzki, T.F., Haff, R.P., Young, R., Can, I., Le, L.C., Toyofuku, N., 1997. Defect detection in apples by means of X-ray imaging. *Trans. ASAE* 40, 1407–1415.
- Studman, C.J., Brown, G.K., Timm, E.J., Schulte, N.L., Vreede, M.J., 1997. Bruising on blush and non-blush sides in apple-to-apple impacts. *Trans. ASAE* 40, 1655–1663.
- Thomas, P., Kannan, A., Degwekar, V.H., Ramamurthy, M.S., 1995. Non-destructive detection of seed weevil-infested mango fruits by X-ray imaging. *Postharvest Biol. Technol.* 5, 161–165.
- Upchurch, B.L., Throop, J.A., Aneshansley, D.J., 1994. Influence of time, bruise-type, and severity on near-infrared reflectance from apple surfaces for automatic bruise detection. *Trans. ASAE* 37, 1571–1575.
- Varith, J., Hyde, G.M., Baritelle, A.L., Fellman, J.K., Sattabongkot, T., 2003. Noncontact bruise detection in apple by thermal imaging. *Innov. Food Sci. Emerg. Technol.* 4, 211–218.
- Veraverbeke, E.A., Verboven, P., Lammertyn, J., Cronje, P., De Baerdemaeker, J., Nicolai, B.M., 2006. Thermographic surface quality evaluation of apple. *J. Food Eng.* 77, 162–168.
- Walczak, R.T., Baranowski, P., Mazurek, W., 2003. Application of thermography in agrophysics. Training Course for Young Research Workers "Physicochemical and Physical Methods of Studies of Soil and Plant Materials. Theory and Practice". IAPAS, Lublin. 27.11–2.12, 111–117 pp.
- Wen, Z., Tao, Y., 2000. Dual-camera NIR/MIR imaging for stem-end/calyx identification in apple defect sorting. *Trans. ASAE* 43, 449–452.
- Więcek, B., Zwolenik, S., 1998. Multichannel thermography systems for real-time and transient thermal process application. In: *Quantitative Infrared Thermography QIRT'98*, pp. 322–325.
- Woolf, A.B., Ferguson, I.B., 2000. Postharvest responses to high fruit temperatures in the field. *Postharvest Biol. Technol.* 21, 7–20.
- Xing, J., Bravo, C., Jancso, P.T., Ramon, H., De Baerdemaeker, J., 2005. Detecting bruises on 'Golden Delicious' apples using hyperspectral imaging with multiple wavebands. *Biosyst. Eng.* 90, 27–36.
- Xing, J., Bravo, C., Moshou, D., Ramon, H., Baerdemaeker, D.J., 2006. Bruise detection on 'Golden delicious' apples by VIS/NIR spectroscopy. *Comput. Electron. Agric.* 52, 11–20.
- Xing, J., Baerdemaeker, D.J., 2007. Fresh bruise detection by predicting softening index of apple tissue using VIS/NIR spectroscopy. *Postharvest Biol. Technol.* 45, 176–183.
- Zion, B., Chen, P., McCarthy, M.J., 1993. Imaging analysis technique for detection of bruises in magnetic resonance images of apples. In: *ASAE Annual International Summer Meeting, Spokane, WA, June 20–23, Paper No. 93-3084*.